

**FUSION OF HYPERSPECTRAL IMAGERY**

William H. Licata, Ph.D.  
 Boeing/Boeing North American  
 Duluth, Georgia 30097  
 William.H.Licata@Boeing.com

**ABSTRACT**

A growing area of interest in the sensor community is the use of measurements made at multiple wavebands to increase the detection and acquisition of low contrast targets. Hyperspectral imagery involves large amounts of high resolution spatial and spectral data which must be processed in a timely manner to assist the decision maker. A lot of this data comes in the form of imagery at different wavebands; an infrared camera, synthetic aperture radar, passive millimeter wave camera or some other sensor. This paper presents a new approach for combining hyperspectral imagery in an efficient manner to significantly reduce the burden on the human or computer decision maker. This technique is based on modern image processing algorithms to create a color image where color is directly related to waveband. Multiple two dimensional images are combined into a single three dimensional image which can be processed in a single processor instead of multiple processors reducing overall sensor cost and complexity. The proposed technique has application to the commercial digital camera market in addition to the military market.

**INTRODUCTION**

There is significant interest in hyperspectral processing in the infrared (IR) community for background suppression and noise reduction to increase the acquisition range and reduce the false alarm rate of infrared sensors. This work is in the relatively early stages of development with efforts concentrating on understanding the basic phenomenon. Applications span missile seekers, threat warning systems and acquisition sensors.

Hyperspectral processing holds the potential for both background suppression and noise reduction. Background suppression is achieved because the target signature changes differently from one spectral band to another compared to background and this can be used as a discriminant for attenuating background energy. Noise is suppressed by exploiting the fact that target is correlated from band to band and noise is uncorrelated. The type of detection processing that is performed depends on whether the sensor is noise limited or background limited for any particular scene. The multiple band images also reduces the likelihood that a target falls on a bad pixel and is not seen at all.

One of the questions being asked by researchers working in the area of hyperspectral processing is whether the multiple sensor data should be combined and then processed or processed and then the processed results combined. This alternate approach to fusing the hyperspectral data is illustrated in Figure 1. Figure 1 (a) illustrates processing followed by fusion while Figure 1(b) illustrates fusion followed by processing. Which approach is best for any application depends on many system requirements. This paper discusses a new technique for combining the sensor data prior to processing, Figure 1(a).

**APPROACHES TO HYPERSPECTRAL DISCRIMINATION**

Hyperspectral discrimination exploits a variation in one of the radiation parameters with wavelength. An example is a rocket plume which emit differently depending on the exhaust gases that make up the plume. Reference 1 list some of the emission bands associated with typical motor exhaust gases. For example, CO emits at  $4.663\mu$ ,  $2.345\mu$  and  $1.573\mu$  so it might be advantageous to center one band

19981123 142

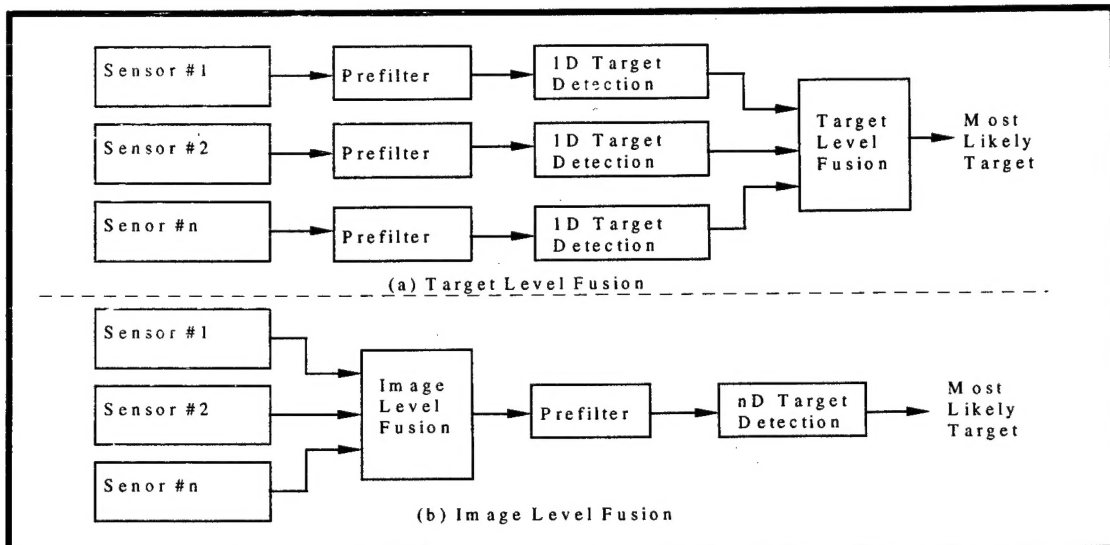


Figure 1. Input Level And Output Level Sensor Fusion

about  $4.663\mu$  and compare it to one at  $3.2\mu$  where CO does not emit. Both these sub-bands are in the midwave region of the IR spectrum. It is expected that the amount of energy in these two sub-bands for any particular pixel will differ depending on whether the pixel contains a rocket plume exhausting CO plus background or background only.

Hyperspectral discrimination is not limited to applications where the target contains exhaust gases of known constituents. The reflectance and emissivity of materials changes with wavelength<sup>1</sup>. If it changes differently for targets materials of interest than it does for background materials, this serves as a discriminant to separate targets from background. This phenomenon is less understood and is a driving reason for building development cameras so a database can be assembled and used to support discrimination algorithm development.

When light interacts with any material it is absorbed, reflected, and scattered. Absorbed energy is ultimately re-emitted as thermal energy in wavelength region that corresponds to the temperature of the material and its absorption spectrum. The infrared emissivity and reflectivity of materials is controlled by both the intrinsic optical properties of the material itself and

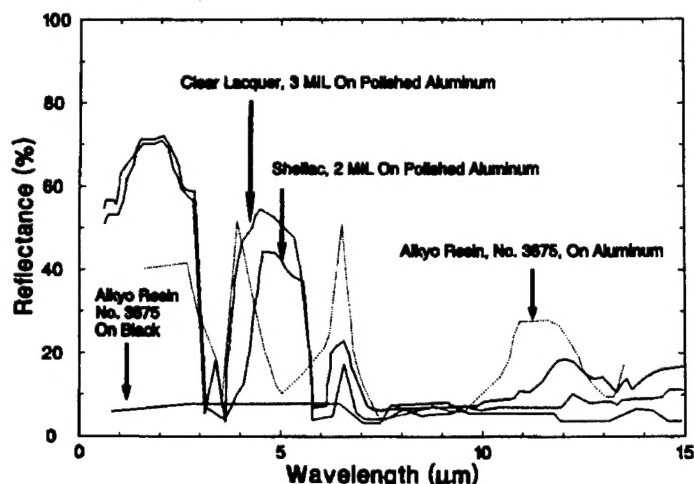
the morphology of the material surface. Typically all reflectivity, absorption, and emission measurements are made on flat samples of the material with polished plane parallel sides. In this case scatter is hopefully minimized and the optical budget for the material can be determined. For low absorbing materials, emission is considered equal to absorption and generally follows the same spectral pattern in the proper thermal wavelength band. For highly absorbing materials and most very hot materials, emission follows a given spectral distribution defined by the temperature of the material which is described as the black body radiation curve. Other partially absorbing materials, or even low absorbing materials with high surface roughness can have an emission spectrum defined by a combination of the material properties and the temperature and these are generally described by the "Gray Body" emission curve.

Trying to identify natural versus man made materials by their emission spectrum is a highly empirical activity. A steel/ ceramic/ alloy vehicle in the woods may have a painted surface that provides the same emission spectrum as wood bark. The main difference may be the angular distribution of the reflected and emitted radiation rather than the spectral distribution, assuming that the tree and the vehicle are at the same

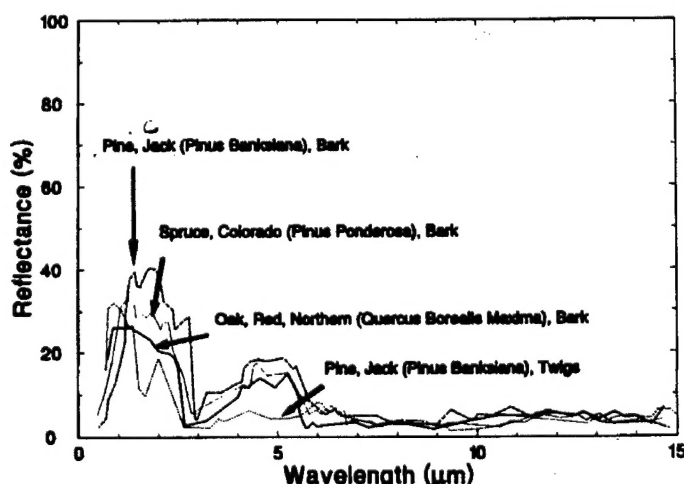
temperature. If the vehicle is hot in reference to it's background it would be easily separated out from the background unless the surface had been painted with a low emissivity material to compensate for the temperature difference.

Figure 2 shows two sets of curves of reflectivity versus wavelength taken from Reference 2. Figure 2(a) was selected since it shows man made objects and Figure 2(b) was selected because it shows natural objects. Significant changes in reflectivity can be seen even within the midwave

infrared band. Notice that some of the metals in Figure 2(a) have a significant response in the long wave band while the trees in Figure 2(b) have a low response in the longwave region. This opens up the possibility that a midwave/longwave sensor may be able to detect a metal object near trees more easily than a single spectral sensor. Further study is required to determine the utility of these changes for acquisition and the best way to exploit any discriminant derived from the changes.



(a)



(b)

Figure 2. Change in Reflectivity with Wavelength (Taken from Reference 2)

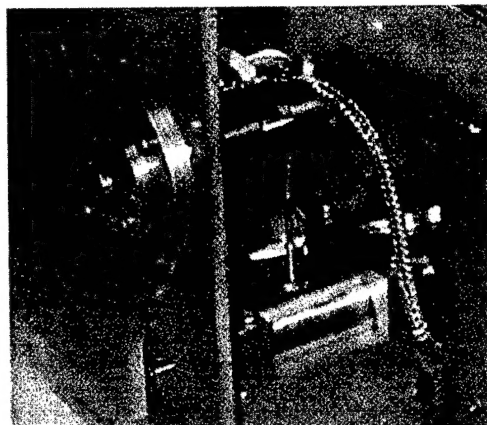


**Figure 3 Hyperspectral Midwave Camera**

Hyperspectral Camera

Figure 3 is a picture of one hyperspectral IR camera. This particular camera uses a 256 x 256 HgCdTe focal plane array integrated with a cryoengine. The lens system uses commercial optics and projects four duplicate images on each of the four 128 x 128 quadrants of the detector array.

By using two separate cold filters inside the dewar, one over each half of the array, simultaneous images can be generated in each of the quadrants of the Focal Plane Array (FPA) as illustrated in Figure 4. The left two images pass thru a spectral filter centered about the lower portion ( $3.87\mu - 4.15\mu$ ) of the midwave band and the right two images through

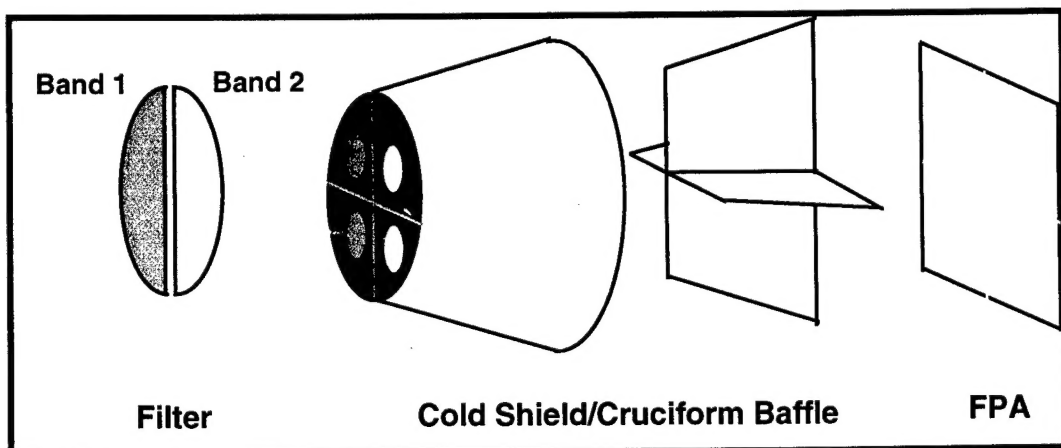


**Figure 4. Lens Design of Development System**

a spectral filter centered around the upper portion of the midwave band ( $4.59\mu - 4.72\mu$ ). A custom lens was designed for this system. The field of view of the lens is on the order of 90 degrees square. It is a diffraction limited design and composed of a single aspheric element. The lens was procured from an optics' vendor and is composed of a 2x2 array of optical elements

on a single optical substrate of silicon. Each lens element is mounted to the dewar and centered over one of the four quadrants of the FPA resulting in a total of four identical images out of the sensor. In order to prevent crosstalk between the channels, a special cruciform cold shield is used inside the dewar assembly along with a pair of semicircular cold filters. Each cold filter

covers half of the focal plane so each half of the plane is looking into one of the two desired wave bands. It was critical that the dewar design be matched to the lens design for this system. This technique of generating multiple band IR imagery can be expanded to cover additional bands, and if the detector array is a dual midwave/longwave sensor, it can cover both the midwave and longwave bands.

The camera electronics uses modifications to existing electronics boards. This primarily involved altering the camera electronics to allow for two sets of calibration coefficients with a 256x256 focal plane array. In addition, minor modifications are required to optimize the display of the video data as well as insuring that the RS422 digital interface is functioning properly. Finally, interface cables interfacing the cryoengine and the preamplifier to the electronics are required.

The software modifications required were to the data collection and the calibration of the two color data. The software design interfaces with some of the electronic

changes to sum multiple frames of data at two different flux levels in order to calculate the gain and offset coefficients for each detector.

The system integration was accomplished in three steps: 1) integrated dewar assembly to electronics, 2) Lens to dewar, and 3) Software verification with lens focus. A custom preamplifier board was built and tested and integrated with the dewar and existing electronics and verified that the dewar cooled and FPA operated as expected. An external filter was also used to verify which band in the image was the red band and which one was the blue one. The lens is connected to the optical train via a precision alignment pin insuring repeatable performance when lens and dewar are attached. A number of changes were made to existing single color software to work with the two color system such as two separate calibrations, blacking out video in quadrants where no image is present to reduce distraction, and modifying software and

electronics to accommodate two separate threshold values (one for each color band).

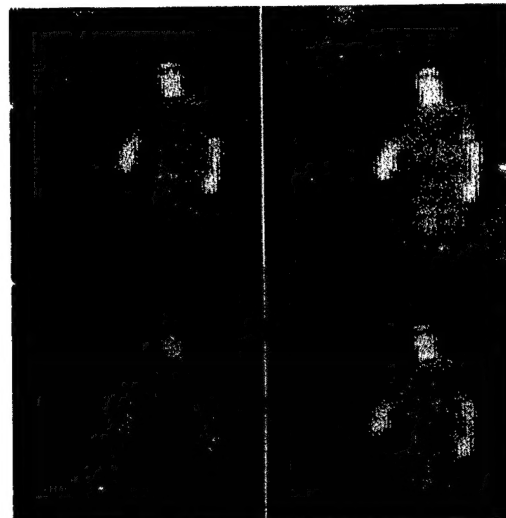


Figure 5. Camera Output Image

#### EXAMPLE OF OUTPUT IMAGERY:

Each 256 x 256 field out of the camera contains four 128 x 128 images as shown in Figure 5. The two hyperspectral images on the top are time coincident and the two on the bottom are time coincident but the top and bottom images differ in time by one half a frame interval. This is because the multiplexer reads the FPA out a row at a time. Each 256 x 256 frame contains two sets of hyperspectral data and one set of temporal data. There is a lot of processing that can be performed on this single frame of data.

#### SPECTRAL DIFFERENCE PROCESSING:

One approach to discriminating targets from background is subtracted from the upper left image from upper right image or lower left from lower right. This gives a measure of change in energy per fixed wavelength change in each pixel. Figure 6a shows the result of subtracting the upper two images and figure 6b the result of subtracting the upper left from the lower right. The subtraction operation involves multiplying one image by a constant so both images have the same mean pixel level, subtracting the two images and then adding 128 so all pixel values are positive. The two images

are different because the two subframes used to generate Figure 6b are not time coincident while those used to generate Figure 6(a) were time coincident. It can be seen in Figure 6a, that the background and

the person gave different residuals pixel intensities implying they changed differently across the sensor waveband.



(a)



(b)

**Figure 6. Difference Images, (1) Upper left from Upper right, (b) Upper left from Lower Right**

#### SPECTRAL AND TIME DIFFERENCING

Spectral differencing of the images doesn't exploit all the information in the images since the image includes both spectral and temporal information. Figure 7 shows the result of computing both the upper and lower

order of the temporal and spectral processing can be reversed and for certain targets, this might give an advantage.

#### Fusion of Multiple Bands at Image Level

The new technique of image level fusion overcomes one of the objections to this approach to generating a hyperspectral camera and that is the loss in spatial resolution since the array has 256x256 pixels but each subpicture has only 128x128 pixels. The image resolution has been halved in both the horizontal and vertical directions. The direct approach to recovering the original resolution requires going to larger arrays or narrower field-of-view optics.

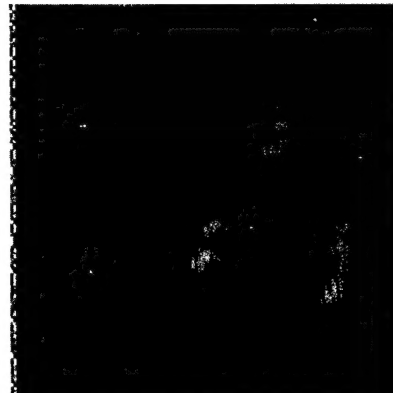


**Figure 7. Spectral-Temporal Processing**

spectral difference images and then differencing these two images which differ in time by one half a field readout time (1/120 sec). This processing approach highlights objects that are moving in waveband and time. In the case of Figure 7, the person's lower arms have a higher intensity than in Figure 6a and the background and body of the person are further suppressed. The

Figure 8 shows what happens when the four images are combined in a simple manner by reordering the pixels so similar pixels are placed next to each other in a composite 256x256 image. The 256x256 looks blurry because there is some misregistration between the four subframes. If adjacent pixels are combined using a weighting filter where the weighting factor is the primary colors, the blurring will be removed and the image will become a color image where

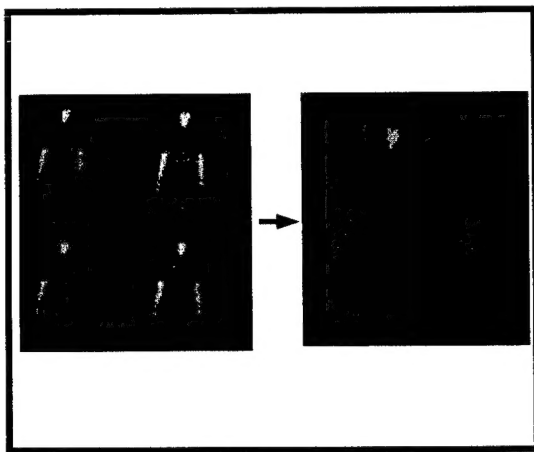


**Figure 8. Fused Hyperspectral Image**  
 color relates to color illustrated in Figure 9. If the four images had been offset from each other by a half pixel shift in different combinations of up, down, right and left, the resulting image would look as if it were created by scanning the array. This suggests that techniques developed for deblurring images could be used for recovering the original 256x256 spatial resolution.

Figure 10 illustrates one way the four images can be combined in support of resolution

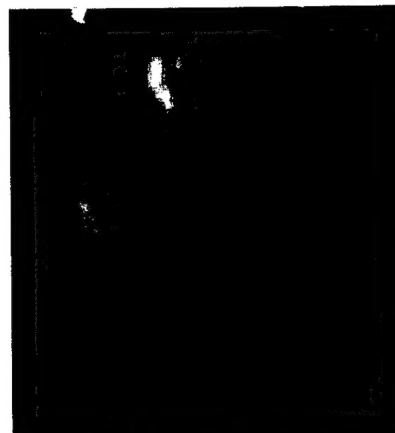


Figure 9 Color Hyperspectral Image

enhancement processing in they were offset by half a pixel. Figure 10 uses the upper left image as a reference for a starting place.

The upper right image is shifted from the upper left image by a half a pixel right. The lower left image is shifted down by half a pixel and the lower right image both a half pixel down and to the right. Pixels in the four images are taken to form new composite pixels as shown in Figure 10. This composite image is a blurred form of any of the four original images. Any of several deblurring algorithms can be used to obtain the desired resolution improvement. The

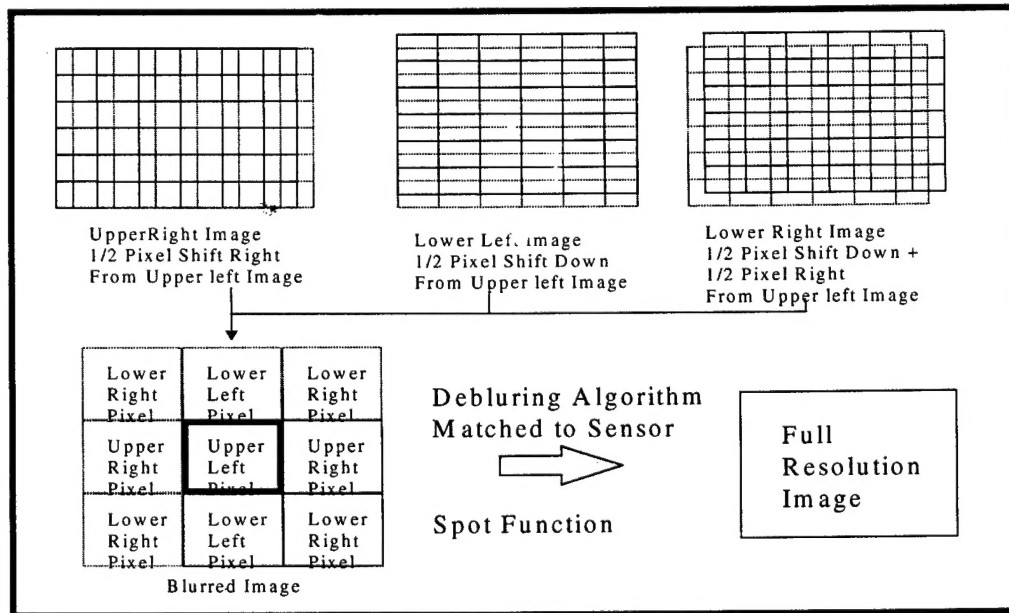


Figure 10 Image Fusion With Resolution Enhancement

pixel shift so the processing cannot be done using the existing imagery. A new camera could provide the overlapping imagery.

#### CONCLUSIONS

A new technique for image level fusion of hyperspectral processing has been presented which makes additional use of the hyperspectral imagery if the images have the required shift with respect to each other. The technique can be expanded to cover as many bands as the sensor can provide. Additional bands (images) benefits the resolution enhancement processing if the image to image shift is adjust to provide additional spatial sampling of the sensor spot function.

#### REFERENCES

1. Wolfe, William L., Handbook of Military Infrared Technology, Naval Research Laboratory, 1965.
2. Zissis, George J., et. Al., The Infrared and Electro-optics Handbook, volume 1, SPIE Optical Engineering Press, 1993.
3. Biemond, et.al., " Iterative Methods for Image Deblurring , " Proceedings of the IEEE, Vol. 78, No. 5, pp 856-882, May 1990